

Dynamics of the ice-age Earth: Solid mechanics and fluid mechanics

W.R. Peltier and L.P. Solheim

Department of Physics, University of Toronto, 60 St. George Street, Toronto, Ontario, Canada M5S-1A7

Abstract. The global theory of the glacial isostatic adjustment process is employed to infer the thicknesses of the continental ice sheets that existed at Last Glacial Maximum 21000 calendar years before present. Further analyses allow the global ice thickness distribution to be mapped into a "paleo-topography" for the planet as a whole, a field that is of primary importance for the understanding, through the application of modern general circulation models, of the surface climate that was characteristic of this epoch of Earth history. Crucial to the success of this procedure is knowledge of the radial visco-elastic structure of the solid Earth. Given an accurate model of the topography of the planet at Last Glacial Maximum that includes the component associated with the distribution of land ice, together with a "surface albedo mask" which differentiates ice covered from non-ice-covered regions, we may proceed to simulate the climate at glacial maximum using a modern coupled atmosphere-ocean general circulation model. Recently obtained results of this program are described which include an initial assessment of the primary modes of climate variability that were characteristic of the glacial state.

1. INTRODUCTION

That there exists, in certain respects, a strong interconnection between processes that occur in the solid-earth component of the Earth System, and the climate that is characteristic of Earth's surface, is a fact that is not always sufficiently appreciated. Probably the best understood of such interconnections is that between surface climate and the processes of mantle convection and continental drift. It is amply understood that climate depends very strongly upon the distribution of land and sea and that this distribution has evolved dramatically as a consequence of continental "drift" during the 4.56 billion years that have passed since the Earth first formed. It is also coming to be understood, at least in general terms, that the concentration of atmospheric carbon dioxide, a vitally important greenhouse gas, has co-varied together with the "Wilson Cycle" of supercontinent creation and destruction. It is very much less well understood, however, that even on much shorter timescales than the 100 million year timescale that is characteristic of the mantle convection process, the solid Earth may play an important role in the determination of surface climate. The best example of this fact concerns the role of glacial isostatic adjustment in mediating the large variations in surface topography that are caused by the massive accumulations of land ice that have occurred during the Pleistocene epoch of Earth history in response to the changes of solar insolation received by the Earth due to changes in the geometry of its' orbit around the Sun. Since the topography of the planet with respect to sea level plays an extremely important role in shaping the general circulations of both the atmosphere and the oceans, it will be clear that the global process of glacial isostatic adjustment may play an important role in shaping surface climate under ice age conditions. The intention of his paper is to present an overview of recent research in what has become an extremely vigorous area of earth-scientific activity.

The modern theory of the glacial isostatic adjustment process was established in a series of papers published in the 1970's [2-7]. In the first three of these articles it was shown how one might construct a normal mode theory for the impulse response of a radially stratified viscoelastic model of the planet to surface mass load excitation. This theory built directly upon the work of Gilbert [e.g. 8] on the normal modes of elastic gravitational free oscillation of the planet which are strongly excited by major earthquakes. There is a strong analogy between the excitation of the normal modes of viscous gravitational relaxation by surface glaciation and deglaciation in the theory that I have developed and this corresponding seismological problem of the excitation of the elastic gravitational free oscillations. In the paper by Farrell and Clark [5] these theoretical elements of the theory of viscous gravitational relaxation were brought together to suggest how one might employ them to compute the variations of relative sea level that are induced by the global process of glaciation and deglaciation that occurred during late Pleistocene time. This methodology was implemented in [6,7] using a primitive initial model of late Pleistocene deglaciation called ICE-1 that had been recorder in the paper by Peltier and Andrews [4]. The viscoelastic model of Earth's interior employed in [6,7] was also rather primitive in that it did not include a lithosphere, and the model of deglaciation did not include an Antarctic component.

Both the theoretical structure employed for the purpose of the computation of the response(s) of the planet to large scale continental deglaciation and the models of this process that are required to implement the theory have been under continuous development at Toronto since this time. In Peltier [9] and Wu and Peltier [10], for example, the further theory was developed that was required to determine the rotational response of the planet to the late Pleistocene glaciation and deglaciation process. These analyses immediately demonstrated that several previously unexplained anomalies in Earth rotation were simultaneously reconciled as consequences of the planet's response to the ice age. These anomalies included the so-called "non-tidal" acceleration of the rate of axial rotation and the "true" polar wander that is currently ongoing at a rate of approximately 1 degree per million years along the 76 degree west meridian. The model of global deglaciation was also improved dramatically with the publication by Tushingham and Peltier [11] of the ICE-3G model. This deglaciation model was further refined in the paper by Peltier [12] who called the refined model ICE-4G, a model that was subsequently employed through application of a formal Bayesian inversion methodology to infer a refinement of the simple VM1 radial viscosity model of [11]. The VM2 model of the radial variation of viscosity was shown to correct systematic misfits of the theory to the observations that had been identified by Tushingham and Peltier at all sites along the east coast of the continental United States, the data from which had not been employed in the formal inversion that delivered VM2 from the starting model VM1. At the same time a new spherical harmonics based methodology was also developed [13] with which to solve the Sea Level Equation, a methodology that has since replaced the rather crude finite element method that was employed in the earlier work of [6].

Progress in the development of this theory of the response of the Earth to global deglaciation has continued over the past decade, with the focus now having shifted to the consideration of additional subtle physical effects that may exert measurable influence at sites remote from the main concentrations of LGM continental ice. Several of these effects derive from the influence of the migration of the coastline that occurs as ice sheets accrete and disintegrate, an accurate global theory for the computation of which was first presented in [12]. In [14] it was shown that the disparity between the eustatic rise of sea level that would have been expected due to the mass of ice whose melting was input to the sea level equation, and the net rise of sea level at sites that would be expected on *a priori* grounds to approximately record the eustatic rise, was due to the action of "implicit ice" that came into play due to the inundation by the sea of sites that were initially ice covered. More recently, in [15, 16] and in [17], it has been shown that the migration of the coastline, in regions where a broad continental shelf is initially exposed by the drop of sea level due to the construction of the LGM ice sheets, one must take careful account of the conservation of mass in computing the water load that is emplaced upon the shelf as it becomes inundated by the sea. This has proven to be especially important in the inference of the eustatic sea level depression that was characteristic of the LGM state [15]. Of similar importance at some locations in the far field of

the ice sheets is the action of the feedback onto sea level due to the changes in Earth rotation that are induced by the process of global glacial isostatic adjustment. Although initially considered too small to be measurable in [18], the unique data set from the southeast coast of the South American continent recently described by Rostami et al. [19] has required that this early impression be modified. Along the coast of Argentinian Patagonia, their data establish the existence of a mid-Holocene high stand of sea level that is 7-8m above the present level of the sea. This would appear to be unprecedented globally, as in most locations this high stand usually has an amplitude that is no more than approximately 3m. Very recently it has been shown in [22] that the unusual amplitude of this feature is a consequence of the action of rotational feedback, the spatial intensity of which has the form of a spherical harmonic of degree 2 and order 1 (see below). Of the 4 extrema in such a pattern, one lies immediately over the southern part of Argentinian Patagonia, thus explaining why rotational feedback should be especially important in this region. Even more recently, analysis of RSL data from the Western Mediterranean Basin has shown that rotational feedback is also important there, although the influence is more subtle still [20].

The conclusion based upon the collectivity of these analyses is that the ICE-4G (VM2) model of the glacial isostatic adjustment process provides an excellent first order description of this phenomenon. This is not withstanding the further refinements that continue to be made to the details of the surface ice distribution and the radial profile of mantle viscosity (e.g. see [21] and [22] for examples concerning the ice distribution). It is therefore expected that the model should prove to be extremely useful as a means of inferring the topography of the planet at Last Glacial Maximum. In the next section of this paper I will briefly review the methodology that is employed to make this inference and describe the results that have obtained thereby. In the subsequent Section of the paper, this topography will be input to a model of the coupled atmosphere-ocean general circulation in order to infer the detailed characteristics of the climate state that obtained during this epoch of Earth history, 21000 years before present.

THEORY: GLACIAL ISOSTASY AND ICE- AGE TOPOGRAPHY

The theory of postglacial relative sea level history is embodied in the Sea Level Equation, an integral equation whose solution consists of the prediction of the history of the separation of the surface of the solid Earth from the surface of the sea (the geoid of classical geodesy) that is induced when ice is removed from the surface of the continents and enters the oceans as water. If we define as $S(\theta, \lambda, t)$ this global time dependent field; in which θ is latitude and λ is longitude, then

$$S(\theta, \lambda, t) = C(\theta, \lambda, t) \left[\int_{-\infty}^t dt' \iint_{\Omega} d\Omega' (L(\theta', \lambda', t') G_{\frac{1}{2}}^+(\gamma, t-t') + \Psi^R(\theta', \lambda', t') G_{\frac{1}{2}}^T(\gamma, t-t')) + \Delta\Phi(t)/g \right]. \quad (1)$$

In (1) the function $C(\theta, \lambda, t)$ is the so-called ocean function which is unity over the oceans and zero over the continents, whereas the field $L(\theta, \lambda, t)$ is the space and time dependent surface mass load which has dimensions of mass per unit area and which has a composite form associated with the fact that it possesses both ice and water components. This form may be represented as

$$L(\theta, \lambda, t) = \rho_I I(\theta, \lambda, t) + \rho_W S(\theta, \lambda, t), \quad (2)$$

in which ρ_I and ρ_W are the densities of ice and water respectively, and I is the space and time dependent ice thickness. The field Ψ^R in (1) is the centrifugal potential perturbation associated with the change in rotation that is caused by the glacial isostatic adjustment process, a field that may be computed given the changes in the three Cartesian components of the angular velocity of the planet that are caused by the GIA process. The latter angular velocity perturbations are determined by the theory of Peltier [9] and Wu and Peltier [10] and the spherical harmonic expansion of the field Ψ^R is expressed in terms of these

components using theory from Dahlen [23]. The remaining functions in (1), namely G_{ϕ}^L and G_{ϕ}^T are Green functions for the surface mass load and gravitational potential load boundary value problems. For the visco-elastic model of the Earth that is required to explain the glacial isostatic adjustment process, these impulse response functions may be constructed using the theory originally developed in Peltier[2]. They are determined solely by the internal viscoelastic stratification of the planet. The final time dependent but space independent term in (1), namely $\Delta\phi(t)/g$, is an adjustment required to ensure that the theoretical prediction of $S(\theta, \lambda, t)$ satisfies the mass conservation constraint that only the water produced by melting ice appears as a load on the ocean basins. It will serve no useful purpose here to provide a detailed review of the mathematical methods that have been developed to construct these elements of the theory, nor to discuss at any length the numerical techniques employed to solve the Sea Level Equation (1). The interested reader will find a reasonably up to date review of this literature in [18].

What will be of interest, however, is the methodology employed to infer the time variation of the topography of the planet with respect to sea level that is induced by the process of glaciation and deglaciation. This requires an adjustment of the field $S(\theta, \lambda, t)$ produced by solving the integral equation (1) in order to ensure its' "topographic self-consistency". This idea, originally developed in [12], arises from the recognition that the field S , being the product of a theory that is accurate only to first order in perturbations from the spherical reference state of the planet, delivers a relative sea level history that is relative to an unspecified and therefore arbitrary datum. This fact may be exploited to develop a prediction of relative sea level history that is consistent with the present day topography of the planet with respect to sea level and a prediction of the evolution of planetary topography through time since last glacial maximum. The procedure is simply as follows. We first introduce a field $T'(\theta, \lambda, t)$ such that

$$S(\theta, \lambda, t_p) + T'(\theta, \lambda) = T(\theta, \lambda, t_p) \quad (3)$$

in which $T(\theta, \lambda, t_p)$ is the present day topography of the solid part of the planet with respect to sea level. I continue to fix T' using the ETOPO5 data base though higher resolution digital topographic data bases now exist which may be employed if higher spatial resolution is desired. Equation (3) therefore determines the field $T'(\theta, \lambda, t)$. Given this field we may then proceed to compute the time dependent topography of the planet with respect to sea level by first computing

$$T_0(\theta, \lambda, t) = S(\theta, \lambda, t) + T'(\theta, \lambda) \quad (4)$$

To this raw estimate of the topography of the rocky part of the planet with respect to sea level we must add the thickness of the ice which covered the surface at time t and at the spatial location with coordinates (θ, λ) . The final prediction of the surface topography at time t in the past is therefore provided by the expression

$$T(\theta, \lambda, t) = T_0(\theta, \lambda, t) + I(\theta, \lambda, t) \quad (5)$$

The northern hemisphere component of the ice distribution at Last Glacial Maximum from which this topography has been derived is shown on Figure 1. In deriving the topography field I I have employed the VM2 model of the internal visco-elastic structure to fix the time dependence of the relaxation process involved in the glacial isostatic adjustment phenomenon. Inspection of Figure 1 will show that the main concentrations of land ice at LGM were located over Canada and over Northwestern Europe. Aside from these primary concentrations of land ice in the Northern Hemisphere, there was also significant ice cover over the mountainous terrain on the southwest coast of the South American continent in a Patagonian ice sheet as well as a significant expansion of the ice cover over Antarctica. A further characteristic of the ice age Earth at Last Glacial Maximum concerns the existence of the land bridges that were exposed by the

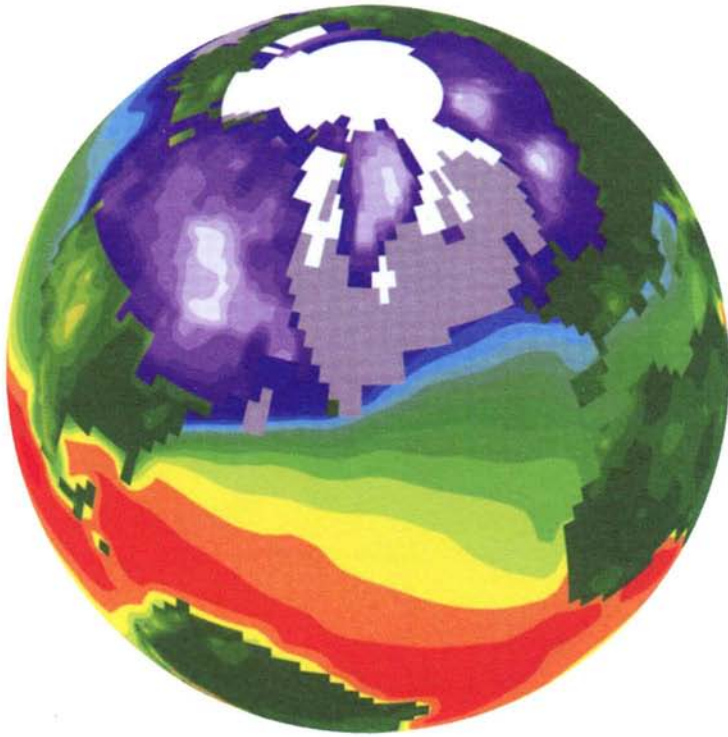


Figure 1. The Northern Hemisphere distribution of ice on the surface of the continents according to the ICE-4G model of [12]. The oceans are coloured according to the annual mean sea surface temperature that is predicted to have obtained under Last Glacial Maximum conditions according to calculations performed with a coupled atmosphere-ocean general circulation model.

fall of sea level associated with ice sheets growth. These land bridges include those in the following regions (see Peltier, 1994 for graphical depictions).

- A. The bridge which then connected Great Britain to the European mainland and to Ireland
- B. The bridge which then connected eastern Siberia to Alaska, the so called continent of Beringia.
- C. The Bridge that connected Australia to New Guinea
- D. The complex network of bridges that was constructed by the exposure of much of the continental shelf in Indonesia.
- E. The incipient bridge that almost formed due to the exposure of much of the continental shelf outboard of the Patagonian shelf of Argentina between the mainland and the Falkland Islands.

The impact of the topography of the planet upon the climate of the Last Glacial Maximum will therefore be felt not only through the increase of continental topography in the regions where the ice sheets existed but also through the increase in the continental area itself, due to the exposure of the continental shelves in areas in which the water which covers them is sufficiently shallow today.

As an example of the predictions that may be made using the ICE-4G deglaciation history shown in Figure 1 when this is employed as input to the Sea Level Equation (1), I show in Figure 2 the prediction of the present-day rate of relative sea level rise obtained when this history of surface loading is used in conjunction with the VM2 model of the radial variation of mantle viscosity. Inter-comparison of Figures 1 and 2 will show that, in regions that were initially covered by continental ice sheets, sea level is

E2g 4f, VM2.PR.cs

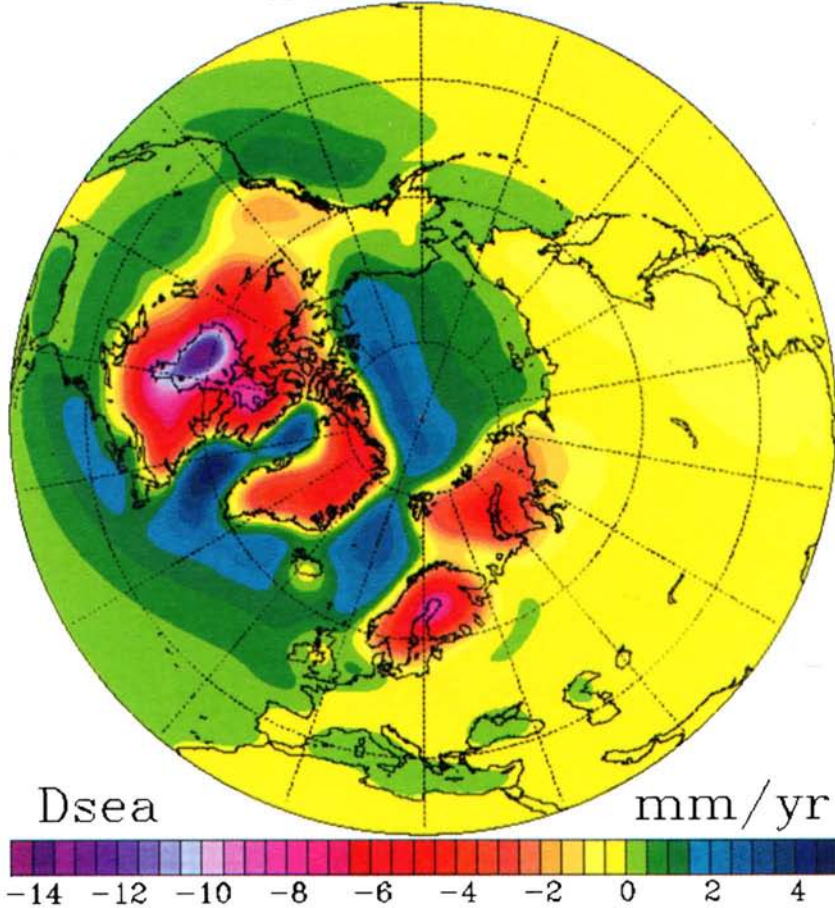


Figure 2. A Northern Hemisphere perspective of the present day rate of relative sea level change predicted by the ICE-4G(VM2) model of the global process of glacial isostatic adjustment when the continental ice distribution shown on Figure 1 is employed as input. The level of the sea is predicted relative to the visco-elastically deforming surface of the solid Earth.

predicted to be falling today since the RSL signal in such regions is dominated by the postglacial “rebound” of the crust of the solid Earth. In the regions exterior to those that were subject to significant glaciation, however, the predicted present-day rate of change of relative sea level is positive, a consequence of the fact that in these regions the signal is dominated by the collapse of the so-called “proglacial forebulge”, an elevation of the surface of the solid Earth produced by the extrusion of mantle material out from under the glaciated region. Upon deglaciation of the initially ice covered regions, the crust in these regions sinks as mantle material flows back beneath the surface of the initially ice covered region in the process of restoring gravitational equilibrium to the coupled solid-Earth-ocean system. It will also be noticed that the present-day rate of sea level rise predicted by the global theory of the glacial isostatic adjustment process remains significant even in the far field of the initially glaciated regions. This turns out to be extremely consequential insofar as the interpretation of the relationship of the present-day rate of global sea level rise to modern greenhouse gas induced climate warming is concerned. Analyses recently reviewed in [24] have shown that when the signal shown on Figure 2 is employed to filter modern tide gauge measurements of secular sea level change, the result is a significant diminution of the

variance in the measurements of the secular rate of change. This work has delivered a best current estimate of the average rate of sea level rise during the 20th century of approximately 1.8 mm per year. Which is to be compared to the estimate from the TOPEX/POSEIDON satellite altimetry based system of 2.4 mm per year. As discussed very recently in Douglas and Peltier [25] and Munk [26], there remains considerable uncertainty as to the ultimate explanation of these inferences. An explanation in terms of the steric effect of thermal expansion of the ocean due to ongoing greenhouse gas induced warming at the surface seems to be ruled out by recently published analyses. Furthermore, the possibility of a significant contribution due to the present-day melting of the great polar ice sheets on Greenland and Antarctica seems to be constrained significantly by the connection of the previously discussed anomalies in Earth rotation to the global process of glacial isostatic adjustment. Although a present-day rate of global sea level rise of order 1 mm per year may be accommodated in the theory simply by elevating the viscosity in the lowermost part of the lower mantle, insofar as the maintenance of the fit to these anomalies is concerned, it remains an issue as to whether one might independently constrain the viscosity and thereby provide a definitive answer to this still open question. One possible means whereby such a definite result might be obtained is through a set of observations that constrain the complete time history of the response of the degree two components of the deformation of planetary shape that is induced by the deglaciation process. Peltier [22] has suggested that this might be possible using the unique set of RSL observations that have been obtained by Rostami et al. [27] from the southeast coast of the South American continent. Further analysis of these data is currently ongoing and could lead to the definitive result that we are seeking.

For the purposes of the present paper, my goal will rather be to exploit the constraints upon planetary topography at glacial maximum that have been obtained through application of the above described theory of the GIA process in order to reconstruct the climate of the Earth that must have obtained during this epoch of earth history. It is to a discussion of this topic that I turn in the following Section.

3. THE CLIMATE OF EARTH AT LAST GLACIAL MAXIMUM I: EXPERIMENTAL DESIGN

The experiments that I will briefly describe herein have been conducted with the Community Climate System Model that has been developed at the US National Center for Atmospheric Research (NCAR), but the integrations of the model that I will describe were performed on the NEC SX-6 vector supercomputer that was recently installed in the Department of Physics at the University of Toronto. The version of this model that I have been employing for this work is the low resolution version in which the model fields are truncated triangularly at degree and order 31 and in which the dynamics of the ocean are described on a 3 degree by 3 degree grid. The atmospheric general circulation model is based upon the spectral transform methodology whereas the ocean model is a grid point model. The interested reader will find a detailed discussion of the components of the model in the collection of papers on it that were published in a special issue of the Journal of Climate (July, 1997). I have been employing a further refined version in which the ocean component has been modified so as to allow an explicit accounting for the El Nino phenomenon [28]. Aside from its' atmospheric and oceanic components, the model includes a reasonably sophisticated sea ice component as well as a somewhat crude representation of land surface processes. An important property of the numerical design is that these 4 primary elements are linked through an intermediate "flux coupler" which serves to transfer information between the model elements. This numerical architecture allows the model to run without having to adjust the fluxes that are passed between elements in order to ensure that the climates that the model delivers in the absence of secular forcing do not drift into unphysical territory.

The experiments that I have performed with this model, in an attempt to obtain the first statistical equilibrium simulations of Last Glacial Maximum climate under ice age conditions, are extremely intensive in their consumption of computer resources, primarily because of the long timescale on which the equilibrium state of the oceans is approached. This timescale being on the order of 1000 years, it will be clear that a fully coupled integration to equilibrium for the coupled system is close to the limit fixed by

available computer resources. To give some idea of the resource requirement, it is perhaps worthwhile to note that using only 4 CPU's on the NEC-SX6 system, the low resolution version of the CCSM will typically deliver 100 years of simulated climate evolution in a single week of continuous integration. On this system, therefore, and restricting the model to accessing only 4 CPU's, a 1000 year integration requires a minimum of 2.5 months of CPU time. The analyses that I will describe herein have yet to reach statistical equilibrium and so they are continuing. However, the integrations are sufficiently close to equilibrium to make the discussion of the results of considerable interest, as I hope will become clear in what follows.

In performing these integrations, a number of modifications were made to the version of the model which has been shown to produce such a good fit to modern climate. The quality of the fit of the CCSM to modern climate observations is of course no guarantee that it will perform in a physically correct fashion when the boundary conditions to which it is subject are changed from those which currently obtain, such as must be done in order to simulate ice age conditions. This is because the numerical structure has been carefully tuned insofar as the parameterization schemes employed to represent sub-grid scale processes are concerned, and there is no guarantee that these representations will remain valid under changed boundary conditions. Accepting this caveat upon the results that are obtained in analyses of this kind, the following adjustments were made to the input parameters in order to simulate the climate at glacial maximum:

- I. The planetary topography with respect to sea level was adjusted using the methodology described in Section 2 of this paper, including the land-sea mask, and including the surface albedo field that is of course strongly modified by the presence of the vast northern hemisphere ice sheets that were in place at this time (see Figure 1).
- II. The seasonal variation of insolation at the top of the atmosphere was adjusted to reflect the impact of the changes in eccentricity and obliquity from present that were then characteristic due to the evolution of the geometry of Earth's orbit around the Sun. The position the solstices and equinoxes were also adjusted to reflect the impact of axial precession. Figure 3 illustrates the LGM insolation regime which will be observed to differ only modestly from present.
- III. The concentrations of the primary radiatively active atmospheric trace gases, CO_2 , CH_4 and N_2O were also adjusted so as to accord with the levels inferred on the basis of measurements made on air bubbles trapped in the ice of the Vostock ice core. This variation in trace gas concentrations provides a critical mechanism whereby the cooling that is driven primarily by processes occurring in the northern hemisphere is exported into the southern hemisphere.

The spin-up of this model to equilibrium was accomplished in a series of steps that also involved two distinct changes in the computer system employed to perform the integration. An initial integration was carried out using a CRAY J series system and the earliest version of the CCSM which did not resolve ENSO. This model was run for 50 years in fully coupled mode from modern initial conditions with the changes I-III above implemented. The integration was then subjected to a period of accelerated deep water evolution, using the so-called Bryan acceleration scheme, following which a further period of 50 years of fully coupled integration was performed. This result was considered to be highly unsatisfactory as the scheme employed to accelerate the convergence of the temperature field in the abyssal ocean was observed not to conserve energy. The integration was then shifted to a NEC SX-5 system, once this was installed in the Toronto laboratory, and run for several hundred years in fully coupled mode using 4 CPU's. However, the efficiency of this integration was too low to make a run to statistical equilibrium practicable. The integration was then shifted once more to the recently installed SX-6 system and the analysis was restarted with the ENSO resolving version of the code since this became available at the same time as the newest machine was installed. This integration has been running for approximately 1200 simulated years to this point and it is results from this integration that will be described in the next section of this paper.

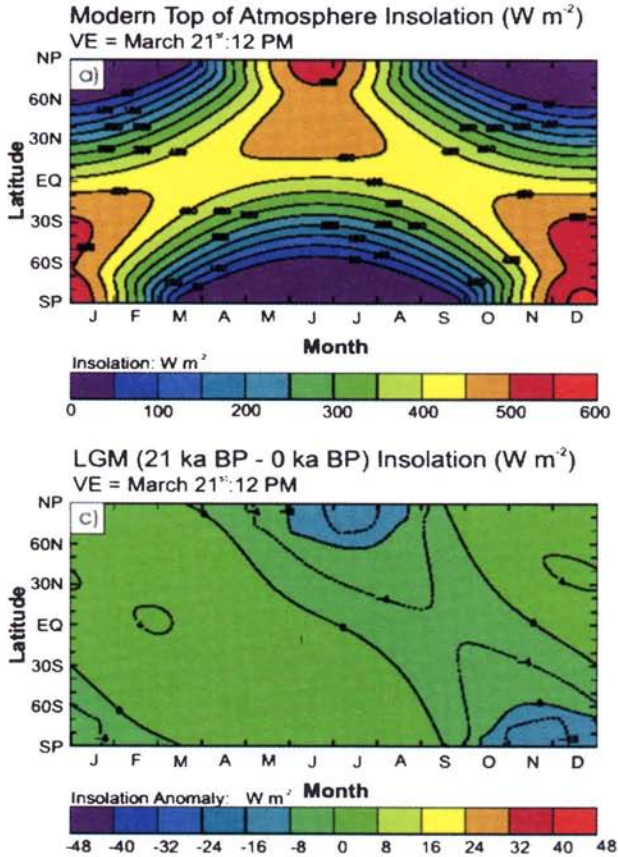


Figure 3. The insolation received at the top of the atmosphere (TOA) as a function of latitude and time of year under modern climate conditions (top) and the deviation of the TOA insolation from modern under Last Glacial Maximum conditions (bottom).

4. THE CLIMATE OF LAST GLACIAL MAXIMUM: RESULTS

Figure 4(a,b) shows a number of fields extracted from this ongoing integration that may be employed as a basis on which to judge the nearness of the calculation to statistical equilibrium. Probably the most sensitive of these fields in this regard is that for the globally averaged temperature of the oceans. Inspection of this field, which is the first in the set shown on Figure 4a, will demonstrate that the model is very close to statistical equilibrium after 1100 years of simulated evolution. Also shown on this Figure is the evolution of globally averaged sea surface temperature, inspection of which will demonstrate that in terms of this field the system has already reached statistical equilibrium. It is of course expected that the temperature of abyssal water will require a significantly longer time to equilibrate than will surface water, since the former is strongly controlled by the deep thermo-haline circulation of the oceans, a long timescale component of the ocean general circulation for which the characteristic timescale for which is of order 1000 years. That the CCSM is delivering a timescale for the approach to statistical equilibrium

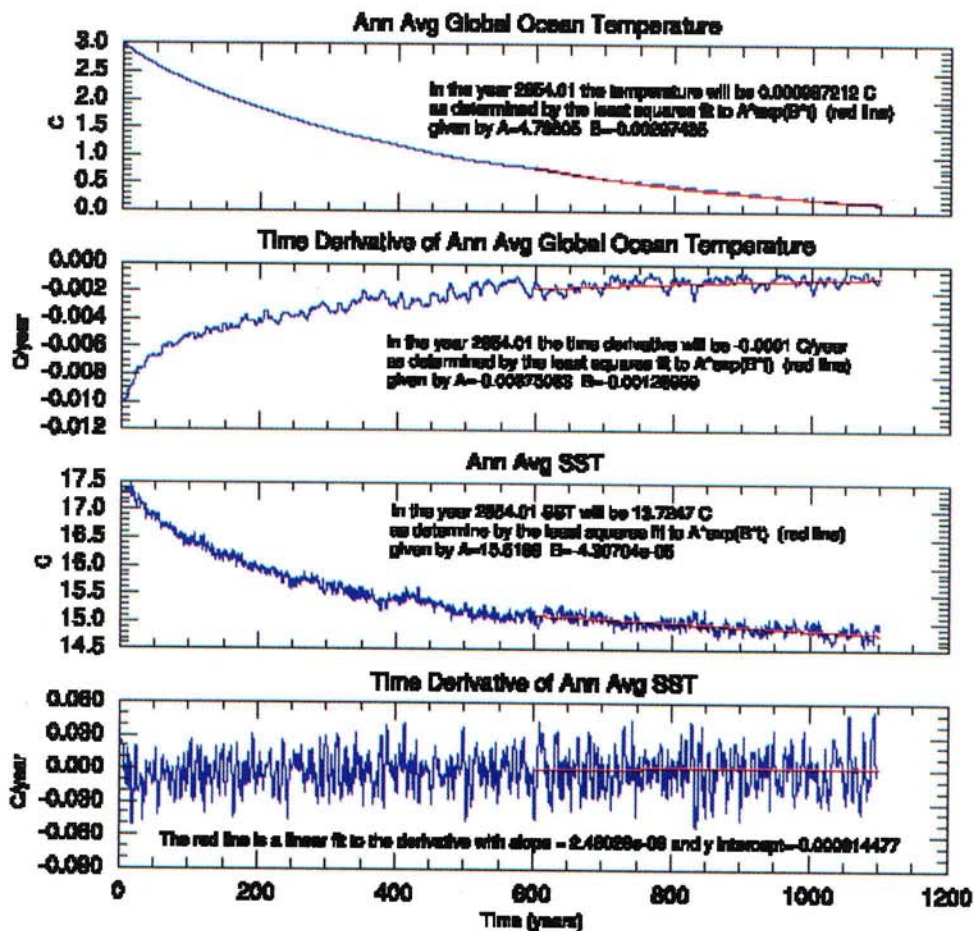


Figure 4. (a) Shows time series for the first 1100 years of the spin-up to equilibrium of the simulation of Last Glacial maximum climate using the NCAR CCSM coupled atmosphere-ocean global climate system model. The time series for which data are shown include the mean temperature of the ocean and its' time derivative and the surface temperature of the ocean and its' time derivative.

that is in agreement with this well established timescale based upon the analysis of the distribution of passive chemical tracers is convincing evidence that the results we are obtaining are not significantly contaminated by "numerical aberration".

Of particular interest then is the evolution of the strength of the meridional overturning stream function in each of the individual ocean basins as this develops during the approach of the model to the statistical equilibrium state. Figure 4b also shows the evolution of these time series. Especially notable in this regard are those for the Atlantic and Southern Oceans which display complementary behavior, indicative of the "sea-saw" effect that has been suggested to be operative based upon the out of phase relationship that has become evident between surface temperature inferences derived from isotopic

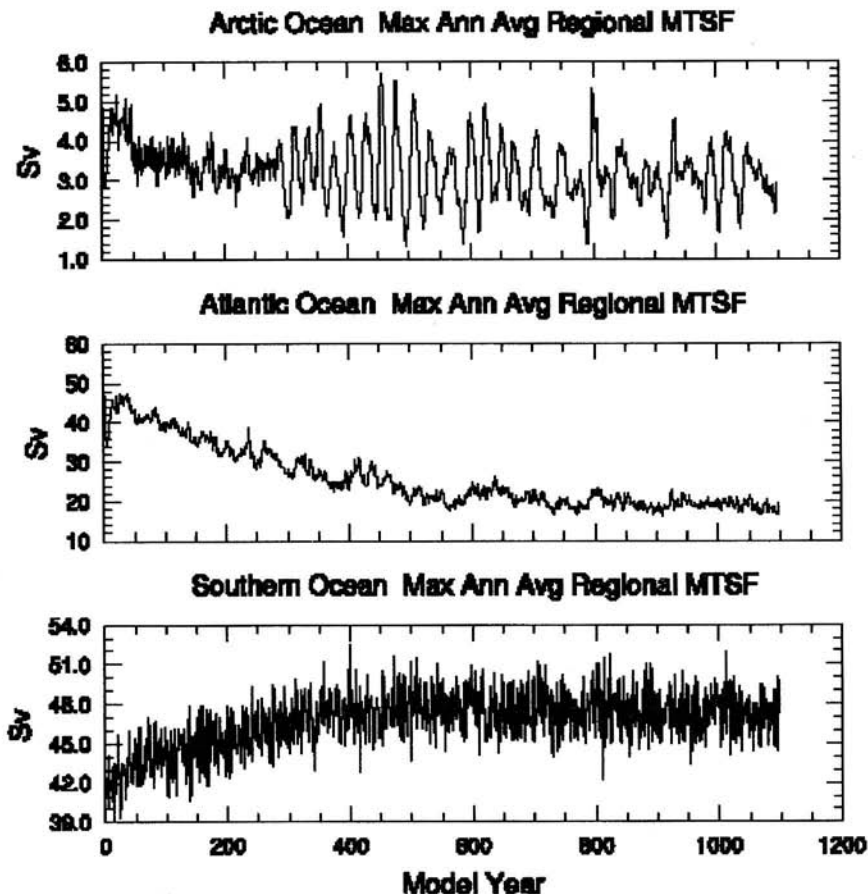


Figure 4. (b) Shows time series of the meridional over-turning stream functions of the Arctic, Atlantic and Southern Oceans during the first 1100 years of the spin-up to equilibrium of the simulation of Last Glacial maximum climate.

measurements from the Greenland (GRIP, GISP2) and Antarctica (Vostock) ice cores. Under glacial maximum conditions the strength of the overturning circulation in the Atlantic is reduced while the strength of the overturning circulation in the Southern Ocean increases. A caveat to the relevance of these results to the actual equilibrium strength of the glacial maximum overturning circulations is that the model does not yet include the additional freshwater flux onto the surface of the North Atlantic Ocean that is known to have been associated with the massive discharges of icebergs that occurred during Heinrich events and it remains unclear (to me) as to whether the glacial maximum ocean is being properly forced in the absence of an accounting for the additional surface freshening that would be associated with the melting of icebergs. It is nevertheless true that no Heinrich event occurred close in time to Last glacial Maximum.

An additional time series shown on Figure 4b is that for the overturning circulation in the Arctic Ocean. Inspection of this result demonstrates the existence of an extremely high degree of variability which clearly begs for a physical explanation. As I will discuss in Subsection 4.3 below, this variability is associated with the North Atlantic Oscillation (NAO) which this model predicts should have been

LGM and MOD Seasonal SST

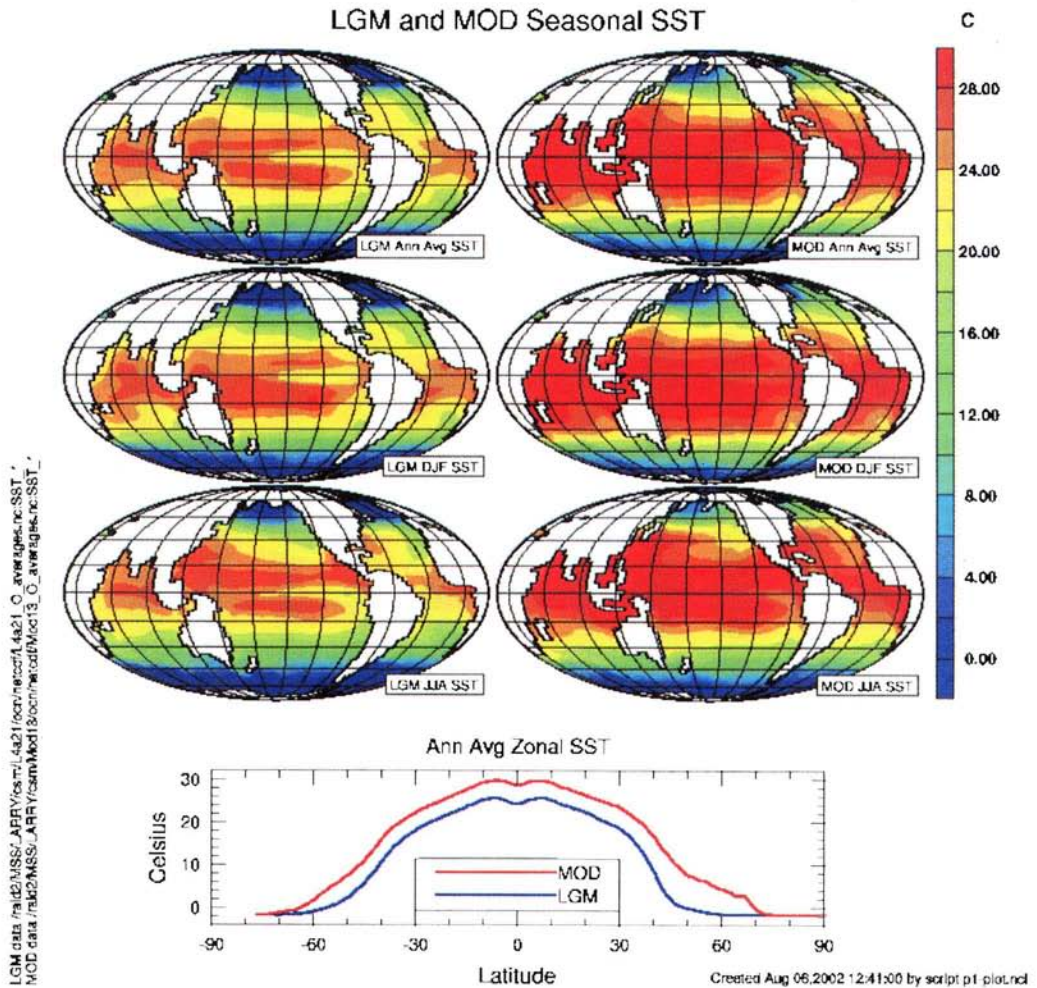


Figure 5. Shows the annually averaged as well as the summer and winter sea surface temperatures from the simulations of both Last Glacial Maximum and Modern climates using the version of the NCAR CCSM model that resolves El Nino. Also shown are the zonally and annually averaged SST's from these two simulations, demonstrating that, in the tropics, SST's are lower than modern by approximately 2.5 degrees Centigrade.

under LGM conditions. As I will demonstrate in what follows this extreme variability in the Arctic Ocean is a consequence of a strongly enhanced North Atlantic Oscillation under the cold climate conditions that obtained during this time. As well as the extremely high quality reproduction of the El Nino process under LGM conditions that the model produces, as we shall see, its' ability to capture the glacial form of the NAO is perhaps of special interest. In the ensuing three Subsections, I will focus sequentially upon different aspects of the LGM climate state that are predicted by these integrations. These concern, respectively, the sea surface temperature in the equatorial region, the form and intensity of ENSO in the equatorial Pacific Ocean, and the form and intensity of NAO in the Northern Hemisphere.

4.1 Tropical sea surface temperatures at last Glacial Maximum

Figure 5 shows both annually averaged and seasonal sea surface temperatures from both the modern control integration and from the integration for Last Glacial Maximum. Also shown is the zonally averaged SST as a function of latitude for both of these integrations of the model. Under LGM

conditions, SST's in the tropics are clearly predicted to be depressed below modern by an average near 2 degrees Centigrade. Comparing the prediction of the LGM model to that of the modern control, it will be noted that the incorporation of ENSO in the calculation leads to an increased depression of SST over a range of a few degrees of latitude centred upon the equator. This is simply explicable as a consequence of the increased strength of the Trade Winds that arises under LGM conditions. The increase in the strength of the tropical easterlies leads to a marked increase in the strength of ocean upwelling off the west coasts of the South American and African continents and therefore to a decrease in SST's in the equatorial Pacific and Atlantic oceans.

This prediction of a depression of tropical SST's by a modest 2-2.5 degrees Centigrade is in close accord with recent measurements based upon the use of the Alkenone proxy (eg. see [29]) but considerably less than the depression earlier inferred on the basis Ca/Sr ratios in corals [30]. It is also close to but somewhat greater than the tropical SST depression originally inferred by the CLIMAP group based upon the analysis of foraminiferal assemblages in deep sea sedimentary cores from the tropical oceans [31]. Other recent analyses based upon coupled atmosphere-ocean models, such as that reported by Hewitt et al. [32] based upon a specially configured version of the UK Hadley Centre coupled atmosphere-ocean model, are in full accord with the result that I have obtained using the fully coupled CCSM. It would appear therefore that the LGM depression of SST in the tropics was rather modest and on the same order as the depression of globally averaged surface temperature over the planet as a whole, the value of which from the present model is approximately 4.0 degrees Centigrade, close to the earliest result for this property of the LGM state originally inferred by Broccoli and Manabe [33] using an early low resolution version of the GFDL model.

4.2 El Nino and the Southern Oscillation at Last Glacial maximum

Conventional ENSO diagnostics from the LGM integration are shown on Figure 6. These consist of four distinct time series, respectively the Equatorial Southern Oscillation Index (EQSOI), and the Nino 4, 3 and 1+2 indices. The SOI is constructed from the surface pressure difference between Tahiti and Darwin Australia and is a measure of the strength of the coupling between the atmosphere and the ocean which is critical to the dynamical processes that sustain ENSO. The remaining indices are all based upon sea surface temperatures, Nino-3 characterizing the temperature of the surface ocean east of 120 degrees west longitude between plus and minus 3 degrees latitude, Nino-4 characterizing the temperature at the sea surface in the warm pool off the east coast of the Australian continent and Nino-1+2 characterizing the temperature of the surface water along the west coast of the South American continent. In Figure 6, each of these indices is shown for a 50 year period for both the model running under pre-industrial climate conditions and under LGM conditions. The pre-industrial data are those recently described in [29]. This inter-comparison demonstrates that the EQSOI exhibits considerably stronger variability under glacial conditions as one might expect given the increased strength of the easterly trade winds that is characteristic of the LGM state. Individual El Nino and La Nina phases of ENSO are both significantly stronger in the cold state than they are under modern conditions. Inspection of the other indices will indicate that the variability of the temperature in the warm pool is not significantly enhanced but that the degree of warming in the surface waters to the east is significantly increased during El Nino phases of the SOI. Because we have over a thousand years of fully coupled integration of an ENSO resolving model we

are clearly in position to construct a composite ENSO event for the glacial period that is highly significant statistically.

Time Series of ENSO Indices

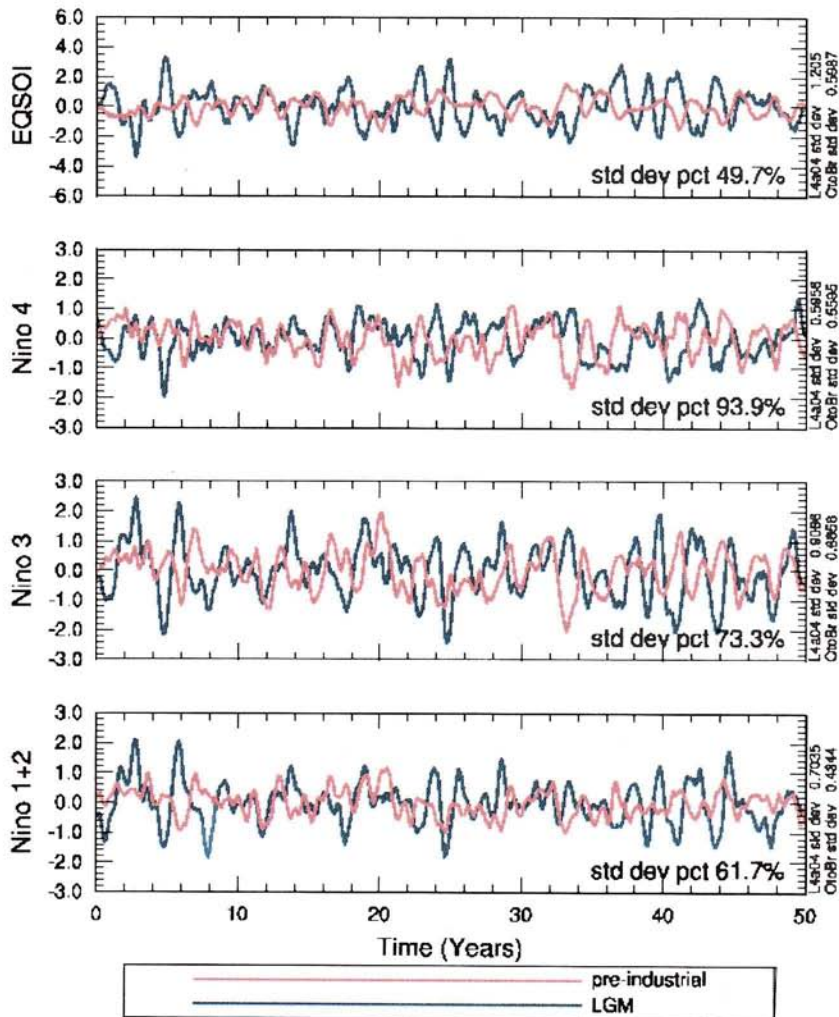


Figure 6. Comparison between the 4 conventional ENSO diagnostics for Last Glacial Maximum and pre-industrial conditions. The diagnostic labeled EQSOI is based upon the normalized pressure difference between Darwin, Australia and Tahiti and is a measure of the strength of atmosphere-ocean coupling. NINO 4 is based upon the temperature of the warm pool in the western equatorial Pacific, NINO 3 is based upon the sea surface temperature along the equator between the west coast of the South American continent and the middle of the Pacific Ocean and NINO 1+2 is based upon the sea surface temperature of South American west coastal waters.

This composite is produced by triggering on maxima of the SOI which are more than 1.5 standard deviations above the mean and superposing the fields in advance and following these epochs by as much as 2.5 years by individual month. According to this criterion we obtain from the 1100 year integration approximately 61 highly significant ENSO events. The composite ENSO produced by the supposition of these events may be characterized in a wide variety of ways, each of which contains dynamically valuable

information from the point of view of understanding the El Nino-Southern Oscillation phenomenon. I will illustrate the results obtained from this compositing procedure by only a single example, that for the evolution of the temperature field as a function of depth and longitude along the equator. This composite is shown on Figure 7. Inspection of this result will demonstrate all of the primary features of the ENSO process. The intense warming of the surface ocean that characterizes “full blown” El Nino conditions off the coast of Peru begins with a depression of the thermocline in the west central equatorial Pacific ocean which appears in the composite as a warming of the water at a depth near 1000m. This tropical thermocline depression thereafter propagates to the east at a speed such that it reaches the west coast of the South American continent on a timescale of order a year. The speed of propagation is not explained by the Kelvin wave speed but rather appears to be a collective property of the nonlinear system. The arrival of the anomaly in thermocline depth at the eastern edge of the Pacific signals the onset of the El Nino phase of the southern oscillation. The composite model result predicts that this occurs during the month of December, as is observed to be the case, El Nino representing a highly nonlinear oscillation of the coupled atmosphere-ocean system that is strongly phase-entrained to the annual cycle of climate variability.

4.3 The North Atlantic Oscillation at Last Glacial Maximum

After El Nino, the mode of natural climate variability that has received most attention recently is that usually referred to as the North Atlantic Oscillation. In comparison with El Nino, which has a characteristic timescale on the order of three to four years, the NAO has a significantly longer timescale of a decade or longer and is therefore best thought of as a mode of inter-decadal variability whereas ENSO is mode of inter-annual variability. This phenomenon is also observed most dramatically in an index defined on the basis of the surface pressure field, in the case of modern climate the (appropriately normalized) difference in pressure between Iceland in the north and the Azores Islands or Gibraltar to the south. This index is essentially a measure of the strength of the northern hemisphere zonal flow over the Atlantic Ocean sector. When the north-south pressure difference is large the zonal flow is strong, when it is small the zonal flow is weak. Based upon the observation that there exists an inter-decadal variability in the NAO index, it is clear that there exists an inter-decadal variability in the zonality of the atmospheric general circulation. Given that the northern hemisphere forcing of stationary planetary waves was significantly different during the glacial period as compared to modern, due both to the mechanical forcing associated with the marked change in surface topography and to the thermal forcing associated with the marked change in surface albedo, one might expect the NAO under glacial conditions to have been rather different from the NAO in the modern climate system. The evidence previously presented concerning the existence of intense variability of the overturning circulation in the Arctic ocean is strongly suggestive of the existence of an intensified NAO at LGM.

The nature of the NAO at LGM may be usefully investigated by creating a composite event in precisely the same way as the ENSO composite was constructed. We first create an NAO index by computing a suitably normalized north-south pressure difference. Under glacial conditions, it turns out that the best choice for the northernmost point of the two employed to construct the index is not Iceland but a rather a point further south. Under modern climate conditions Iceland is near the focus of a low pressure centre in the northern hemisphere. Under glacial conditions, however, this low pressure centre is shifted somewhat to the south as shown on Figure 8. Figure 9 shows the NAO index computed on the basis of this slightly modified choice for the northernmost “Centre of Action”. To create an NAO composite we trigger the construction by choosing those “events” defined by times when the NAO index is more than 1.5 standard deviations above the mean. We then stack and average the field for which we wish to develop the composite NAO event and display the result, in this case, in the form of superimposed annually averaged spatial patterns. Figure 10 shows an example NAO composite for the northern hemisphere surface temperature distribution. Inspection of this result demonstrates that there exists a strong signal surface temperature variability associated with this phenomenon during the glacial period. Given this, it is clearly necessary to think of ice age climate as being more highly variable than

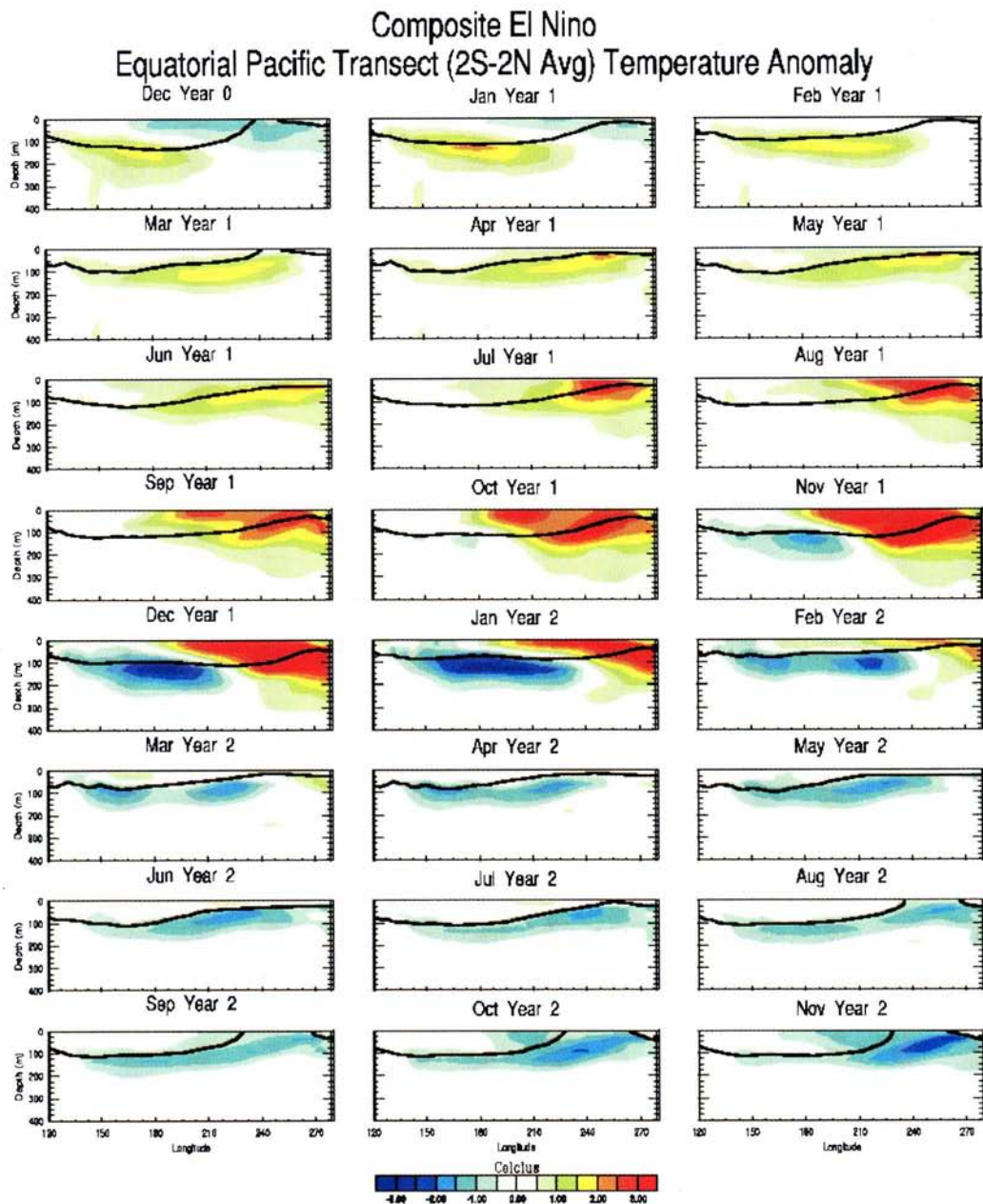


Figure 7. Two years of ocean temperature data for the composite LGM ENSO expressed in terms of monthly averages on a longitude-depth section, with temperature at each point in the section determined by averaging in latitude from -2 degrees south to +2 degrees north. The composite ENSO has been produced by superimposing the 61 most intense events determined on the basis of their strength in the SOI being in excess of 1.5 standard deviations above the mean. Note that the peak strength of El Niño occurs in the month of December, in accord with observations of this phenomenon.

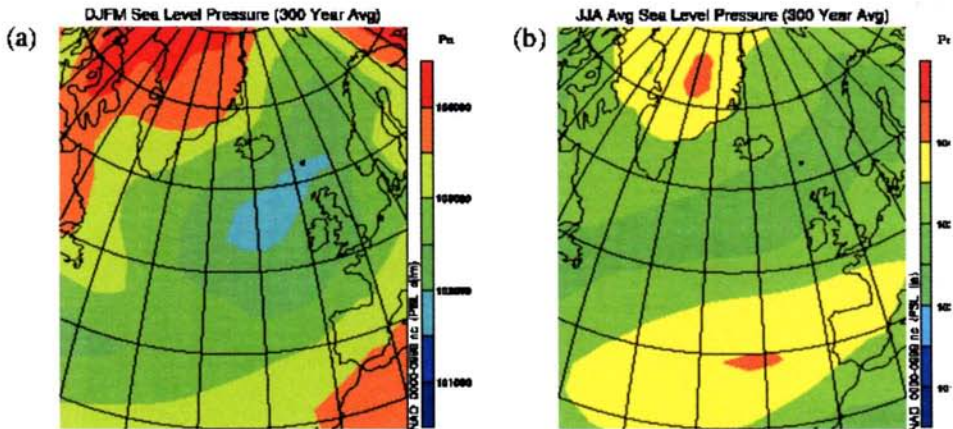


Figure 8. The North Atlantic Oscillation Index at LGM is determined as the normalized difference in sea level pressure between the area (35N-45N, 30W-15W) and (50N-60N, 25W-10W). These areas are summer max (lower frame) and winter min (upper frame) of the annual average sea level pressure. Note that the present day NAO index is determined as the normalized difference in sea level pressure between the Azores and Iceland. The southern point (Azores) remains the same but the northern point is shifted south of Iceland by 5-10 degrees.

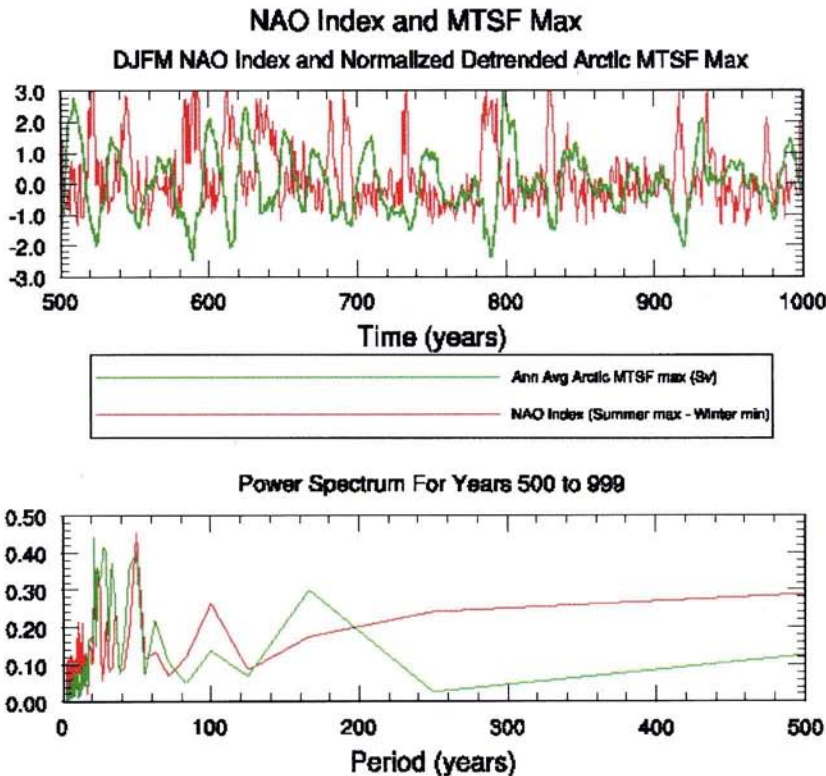
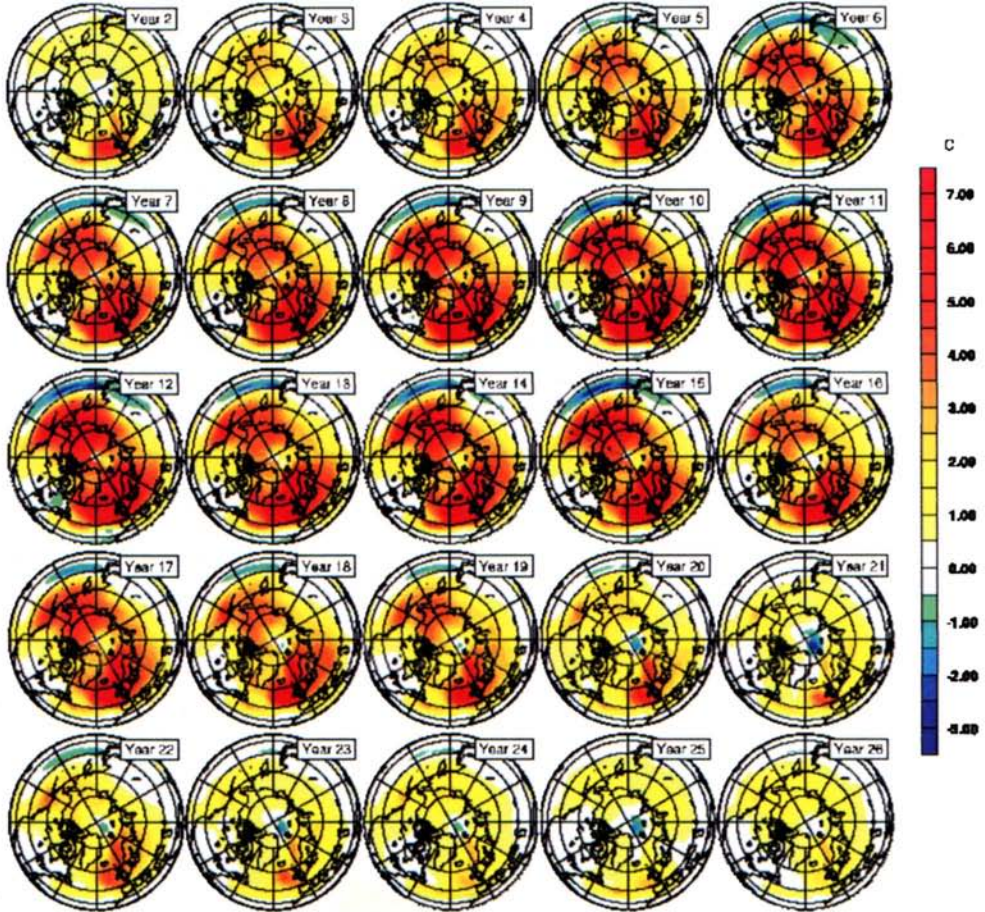


Figure 9. Variations in the NAO index (read curve) and variations in the Arctic meridional transport streamfunction (green curve) are anti-correlated to a high degree. This is most noticeable during the large amplitude excursions such as those clustered around 600 years or around 800 years. Data for these figures was taken from the last 500 years of the 1000 year LGM approach to equilibrium simulation. (figure created by script NAO-plot.nc).

NAO Composite Ann Avg Surface Air Temperature Anomaly



data /raid2/MSS/LARRY/csm/plot-L/NAO_0000-0999.nc (1000 model years)

figure created by script NAO-plot.nc May 15,2002 14:23:58

Figure 10: Composite North Atlantic Oscillation under LGM climate conditions derived from the 1100 year spin-up of the NCAR CCSM model. This composite is in terms of Northern Hemisphere annually averaged surface temperature, inspection of which will reveal that the NAO under glacial conditions consists of an almost annular mode of surface temperature variation, with the annular character broken only slightly by the presence of the continents.

present, not only in terms of inter-annual variability but also in terms of inter-decadal variability. This fact is extremely important to keep in mind when one interprets paleo-data based reconstructions of climate state. Insofar as the surface temperature composite for the LGM NAO is concerned, the reconstruction provides strong evidence that the CLIMAP reconstruction of LGM surface conditions, which included a strong suggestion of enhanced sea ice concentration along the eastern Atlantic margin as far south as Spain, could very well be correct. According to the LGM NAO sea ice fraction composite (not shown here), the existence of high concentrations of sea ice in this region was a consequence of the intense NAO that was characteristic of glacial conditions.

5. CONCLUSIONS

In order to reconstruct climates of the distant past, one requires accurate information concerning not only the solar insolation regime to which the planet was subject, but also the concentrations of radiatively active trace gases as well as the topography and albedo of the surface itself. The science of solid Earth geodynamics may aid enormously in providing information concerning surface topography during the most recent million years or so of Earth history because the global theory of glacial isostatic adjustment has been refined to a sufficient degree as to be extremely useful in this regard. In this paper I have brought together the results inferred concerning surface topography at Last glacial Maximum 21000 years before present with the tools of modern computational climatology to illustrate the power of this combination of perspectives. Of greatest interest are the new insights being achieved in understanding the natural climate variability that must have existed under ice-age conditions. The numerical results being obtained in this program of research are proving to be extremely useful in aiding in the design of appropriate reduced models of both the ENSO and NAO processes, models which are based upon notions from the theory of dynamical systems.

Acknowledgements

I am grateful to Larry Solheim, Guido Vettoretti, Rosemarie Drummond and Ana Sousa for their assistance in the preparation of this manuscript during a portion of my sabbatical leave at the Institut de Physique du Globe de Paris. I also wish to express my thanks to the Director of the Institute, Professor Claude Jaupart, for his hospitality during my stay.

References

- [1] Peltier W.R., Earth system history, in *The Encyclopedia of Global Environmental Change*, M.C. McCracken and J.S. Perry eds., pp. 31-60, John Wiley and Sons, 2002.
- [2] Peltier W.R., *Rev. Geophys.* 12 (1974) 649-669.
- [3] Peltier W.R., *Geophys. J.R.A.S.* 46 (1976) 669-706.
- [4] Peltier W.R. and Andrews J.T. *Geophys. J.R.A.S.* 46 (1976) 605-646.
- [5] Farrell W.E. and Clark J.A. *Geophys. J.R.A.S.* 46(1976) 647-667.
- [6] Clark J.A., Farrell W.E. and Peltier W.R. *Quat. Res.* 9(1978) 265-287.
- [7] Peltier W.R., Farrell W.E. and Clark J.A. *Tectonophys.* 50(1978) 81-110.
- [9] Peltier W.R. *Adv. Geophys.* 24(1982) 1-146.
- [10] Wu P. and Peltier W.R. *Geophys. J.R.A.S.* 76(1984) 202-242.
- [11] Tushingham A.M. and Peltier W.R. *J. Geophys. Res.* 96(1991) 4497-4523.
- [12] Peltier W.R. *Science* 265 (1994) 195-201.
- [13] Mitrovica J.X. and Peltier W.R. *J. Geophys. Res.* 96(1991) 20053-20071.
- [14] Peltier W.R. *Geophys. Res. Lett.* 25(1998) 3957-3960.
- [15] Peltier W.R. *Quat. Sci. Rev.* 21(2002) 377-396.
- [16] Peltier W.R. *Quat. Sci. Rev.* 21(2002) 409-414.
- [17] Peltier W.R. and Drummond R. *Geophys. Res. Lett.* April 15, 2002.
- [18] Peltier W.R. *Rev. Geophys.* 36(1998) 603-689.
- [19] Rostami K., Peltier W.R. and Mangini A. *Quat. Sci. Rev.* 19(2000) 1495-1525.
- [20] Peltier W.R., Pirazzoli P. and Morhange C. *Earth Planet. Sci. Lett.*, submitted, 2002.
- [21] Tarasov L. and Peltier W.R. *Geophys. J. Int.*, July 2002.
- [22] Peltier W.R. *J. Quat. Sci.*, in press, 2002.

- [23] Dahlen F.A. Geophys. J.R.A.S. 46(1976) 363-406.
- [24] Peltier W.R. in Sea Level Rise, B.C. Douglas, M.S. Kearney and S.P. Leatherman, eds., 2001.
- [25] Douglas B.D. and Peltier W.R. Physics Today 55(2002) 35-40.
- [26] Munk W. PNAS USA 99(2002) 6550-6555.
- [27] Rostami K., Peltier W.R. and Mangini, A. Quat. Sci. Rev. 19(2000) 1495-1525.
- [28] Otto-Bliessner B. and Brady E. C. J. Climate 14(2001) 3587-3607.
- [29] Broecker W.S. The Glacial World According to Wally, Eldigeo Press, 1995, 318.pp.
- [30] Guilderson T.P., Fairbanks R.G. and Rubenstone J.L. Science 263 (1994) 663-665.
- [31] CLIMAP Project Members Science 191(1976) 1131-1137.
- [32] Hewitt C.D, Broccoli A.J., Mitchel J.F.B. and Stouffer R.J. Geophys. Res. Lett. 28(2001) 1571-1574.
- [33] Broccoli A.J. and Manabe S., J. Geophys. Res. 90(1985) 2167-2190.